Journal of the Optical Society of America A

OPTICS, IMAGE SCIENCE, AND VISION

Partially coherent vortex beams of arbitrary order

C. S. D. STAHL AND G. GBUR*

Department of Physics and Optical Science, UNC Charlotte, Charlotte, North Carolina 28223, USA
*Corresponding author: gjgbur@uncc.edu

We derive analytic solutions for an infinite set of partially coherent vortex beams (PCVBs) of any azimuthal order and for any propagation distance. The correlation singularities of the beams and their orbital angular momentum are investigated. This detailed study of PCVBs opens the possibility of using such beams for remote sensing and free-space optical communications.   © 2017 Optical Society of America

OCIS codes: (030.1640) Coherence; (050.4865) Optical vortices; (260.6042) Singular optics.

https://doi.org/10.1364/JOSAA.34.001793

1. INTRODUCTION

There has been increased recognition in recent years that singular optics [1,2], as a relatively unexplored area of classical electromagnetism, holds great potential for new and innovative technologies. This research area largely focuses on structures known as *optical vortices*, which manifest as lines of zero amplitude in 3D space on which the phase of the field is undefined (or singular) and around which the phase circulates. Besides being of physical interest, fields with vortices have properties that have been considered for a variety of practical techniques. They have now been employed in multiple applications including optical trapping [3], coronagraphy [4], spatial and temporal coherence filtering [5], phase contrast microscopy [6], and free-space optical communication [7].

While much of the present work has explored the properties of fully coherent light, there are several practical considerations that encourage the use of partially coherent light. For example, partially coherent light has been shown to be more resistant to degradation on propagation through a turbulent medium than its fully coherent counterpart [8], making it of interest for free-space optical communication. When used in imaging, partially coherent light leads to less speckle [9].

However, there are a number of conceptual challenges that arise when dealing with vortices in partially coherent light that are not present in the fully coherent case, among them the lack of a definite phase for fields that are not spatially coherent [10]. Researchers have instead investigated phase singularities in the two-point correlation functions of partially coherent fields to better understand the relation between coherence and vortices. Such singularities have been studied theoretically [11–13] and experimentally [14–17]; these structures are now called *correlation singularities*, which are analogous to and related to coherent optical vortices [18]. Beams with correlation singularities may be particularly useful for the aforementioned free-space optical communications, where the stability of this class of

vortices is of great interest, as a major hurdle for such technologies has been the loss of information in free-space transfer.

At present, while it has been shown that optical and correlation singularities produced by a system are related, the understanding of that relationship remains limited, in no small part due to the complicated nature of correlation singularities. Because correlation functions characterize the field fluctuations between two points in space, twice the number of variables is required per spatial dimension considered. A 2D description requires four variables and a 3D description requires six. There has been a large body of work exploring PCVBs with a first order vortex in a 2D transverse plane [19–21], and we have previously published the full solution for a propagating first order PCVB in six variables [22]. The only other recent work on partially coherent Laguerre–Gauss beams as a class used an elaborate modal construction and did not explore their vortex structures or correlation singularities [23].

In this paper, we determine a generalized solution for partially coherent Laguerre–Gauss beams of radial order zero. The result is a new infinite set of partially coherent vortex beams whose propagation and statistical properties can be described analytically. By considering the case where the radial order $n = 0$ and the azimuthal order $m \in \mathbb{Z}$, we are able to gain new insight into the behavior of such partially coherent Laguerre–Gauss beams, including a description of their orbital angular momentum characteristics, and can better evaluate their suitability for a variety of applications.

2. CALCULATION

When working with partially coherent beams, it is mathematically convenient to work in the frequency domain with the cross-spectral density function $W(\mathbf{r}_1, \mathbf{r}_2, \omega)$, which can be expressed as [24]

$$W(\mathbf{r}_1, \mathbf{r}_2, \omega) = \langle \tilde{U}(\mathbf{r}_1, \omega) U(\mathbf{r}_2, \omega) \rangle_\omega, \tag{1}$$

where $\langle \cdots \rangle_\omega$ represents an average over an ensemble of monochromatic fields. We use a tilde to represent the complex conjugate for notational convenience throughout the paper. As the complete spatial coherence properties of a quasimonochromatic field centered at ω_0 are well-approximated by the value of the cross-spectral density at ω_0, we will suppress ω for brevity, and assume a quasimonochromatic field.

We begin with the equation for a monochromatic Laguerre–Gauss beam of radial order 0, azimuthal order $\pm m$, with $m \geq 0$. Such a wave field can be written as

$$U(x, y, z) = C(x \pm iy)^m \exp\left[-\frac{1}{\sigma^2}(x^2 + y^2)\right] \exp[-i\omega t], \tag{2}$$

where

$$C \equiv \sqrt{\frac{2}{\pi w_z^2 |m|!}} \left(\frac{\sqrt{2}}{w_z}\right)^{|m|} \exp[-i\Phi(z)]. \tag{3}$$

In these expressions, $\Phi(z)$ represents the Gouy phase shift, while σ is defined as

$$\frac{1}{\sigma^2} = \frac{1}{w_z^2} + \frac{ik}{2R_z}. \tag{4}$$

The quantity w_z is the beam width at propagation distance z, defined by

$$w_z = w_0 \sqrt{1 + \left(\frac{z}{z_R}\right)^2}, \tag{5}$$

with w_0 the width of the beam in the waist plane $z = 0$. The quantity R_z is the radius of curvature

$$R_z = z\left[1 + \left(\frac{z_R}{z}\right)^2\right]. \tag{6}$$

Finally, we note that $k = \omega/c = 2\pi/\lambda$ is the wavenumber of the light wave, and $z_R = \pi w_0^2/\lambda$ is the Rayleigh range of the beam.

In discussing correlation singularities, we restrict ourselves to the case where both $\mathbf{r}_1$ and $\mathbf{r}_2$ reside in the same transverse z plane, i.e., $z_1 = z_2 \equiv z$, since it was shown in [22] that singularities only appear in this case. We can use Eq. (2) to generate mth-order partially coherent beams from a so-called beam wander model [20], which describes a partially coherent beam as a Laguerre–Gauss beam propagating in the z direction with a central axis which is a random function of transverse position. This model may be realized with a cross-spectral density of the form

$$W(\mathbf{r}_1, \mathbf{r}_2) = \int \tilde{U}(\mathbf{r}_1 - \mathbf{r}_0)U(\mathbf{r}_2 - \mathbf{r}_0)f(\mathbf{r}_0)d^2\mathbf{r}_0, \tag{7}$$

where $\mathbf{r}_0$ is the transverse position of the axis. We assume the axis position is randomly distributed as a Gaussian:

$$f(\mathbf{r}_0) = \frac{1}{\pi\delta^2} \exp\left[\frac{-(x_0^2 + y_0^2)}{\delta^2}\right], \quad \text{with } \mathbf{r}_0^2 = x_0^2 + y_0^2. \tag{8}$$

As $f(\mathbf{r}_0)$ is a probability density, it has been normalized such that the integral over the entire transverse plane is equal to unity. Here δ is a coherence parameter indicating the RMS wander of the axis; a large value of δ corresponds to more

wander and consequently lower spatial coherence. Thus we may write the cross-spectral density integral as

$$W(\mathbf{r}_1, \mathbf{r}_2) = \frac{|C|^2}{\pi\delta^2} \int [(x_1 - x_0) \mp i(y_1 - y_0)]^m$$
$$\times [(x_2 - x_0) \pm i(y_2 - y_0)]^m$$
$$\times \exp\left\{-\frac{1}{\tilde{\sigma}^2}[(x_1 - x_0)^2 + (y_1 - y_0)^2]\right\}$$
$$\times \exp\left\{-\frac{1}{\sigma^2}[(x_2 - x_0)^2 + (y_2 - y_0)^2]\right\}$$
$$\times \exp\left\{-\frac{x_0^2 + y_0^2}{\delta^2}\right\} dx_0 dy_0. \tag{9}$$

This integral can be solved analytically by judicious use of the binomial theorem, which allows us to reduce it to a sum of integrals of Gaussian form with known solutions. Those not interested in the lengthy derivation can skip directly to the result [Eq. (27)].

We begin by completing the square with respect to x_0 and y_0 in the exponents, with the introduction of the quantities

$$A \equiv \frac{1}{\tilde{\sigma}^2} + \frac{1}{\sigma^2} + \frac{1}{\delta^2} = \frac{2}{w_z^2} + \frac{1}{\delta^2}, \tag{10}$$

$$B_x \equiv \left(\frac{x_1}{\tilde{\sigma}^2} + \frac{x_2}{\sigma^2}\right), \tag{11}$$

$$B_y \equiv \left(\frac{y_1}{\tilde{\sigma}^2} + \frac{y_2}{\sigma^2}\right). \tag{12}$$

The result puts the cross-spectral density into the form

$$W(\mathbf{r}_1, \mathbf{r}_2) = \frac{|C|^2}{\pi\delta^2} \exp[B_x^2/A] \exp[B_y^2/A]$$
$$\times \exp\left\{-\frac{1}{\tilde{\sigma}^2}[x_1^2 + y_1^2]\right\} \exp\left\{-\frac{1}{\sigma^2}[x_2^2 + y_2^2]\right\}$$
$$\times \int [(x_1 - x_0) \mp i(y_1 - y_0)]^m [(x_2 - x_0) \pm i(y_2 - y_0)]^m$$
$$\times \exp[-A(x_0 - B_x/A)^2] \exp[-A(y_0 - B_y/A)^2] dx_0 dy_0. \tag{13}$$

The exponential factors outside of the integral do not significantly affect the phase structure of the field; for brevity, we combine them into a new function:

$$D(\mathbf{r}_1, \mathbf{r}_2) \equiv \frac{|C|^2}{\pi\delta^2} \exp\left[-\frac{1}{\tilde{\sigma}^2}\rho_1^2\right] \exp\left[-\frac{1}{\sigma^2}\rho_2^2\right]$$
$$\times \exp[B_x^2/A] \exp[B_y^2/A], \tag{14}$$

with $\rho_1^2 = x_1^2 + y_1^2$, and a similar expression for ρ_2^2. We now make the coordinate transformation,

$$X \equiv x_0 - \frac{B_x}{A}, \tag{15}$$

$$Y \equiv y_0 - \frac{B_y}{A}, \tag{16}$$

and introduce the notation

$$H_j^{\pm} \equiv x_j \pm iy_j - \left(\frac{B_x}{A} \pm i\frac{B_y}{A}\right), \qquad j = 1, 2. \tag{17}$$

Our integral for the cross-spectral density then takes on the relatively simple form

$$W(\mathbf{r}_1, \mathbf{r}_2) = D(\mathbf{r}_1, \mathbf{r}_2) \int [H_1^{\mp} - (X \mp iY)]^m \exp[-AX^2]$$
$$\times [H_2^{\pm} - (X \pm iY)]^m \exp[-AY^2] dXdY. \tag{18}$$

This integral is still too difficult to directly evaluate. We may now, however, apply the binomial expansion twice to the integrand, such that

$$[H_1^{\mp} - (X \mp iY)]^m = \sum_{k=0}^{m} \binom{m}{k} (-H_1^{\mp})^{m-k} (X \mp iY)^k, \tag{19}$$

$$[H_2^{\pm} - (X \pm iY)]^m = \sum_{l=0}^{m} \binom{m}{l} (-H_2^{\pm})^{m-l} (X \pm iY)^l. \tag{20}$$

We then have

$$W(\mathbf{r}_1, \mathbf{r}_2) = D(\mathbf{r}_1, \mathbf{r}_2) \sum_{k=0}^{m} \sum_{l=0}^{m} \binom{m}{k} \binom{m}{l}$$
$$\times \int (-H_1^{\mp})^{m-k} (X \mp iY)^k \exp[-A(X^2 + Y^2)]$$
$$\times (-H_2^{\pm})^{m-l} (X \pm iY)^l dXdY. \tag{21}$$

We now note that the integrand has rotational symmetry about the (X, Y) origin. By moving into polar coordinates such that

$$X + iY \equiv \rho e^{i\phi}, \tag{22}$$

we can further simplify the integral to the form

$$W(\mathbf{r}_1, \mathbf{r}_2) = D(\mathbf{r}_1, \mathbf{r}_2) \sum_{k=0}^{m} \sum_{l=0}^{m} \binom{m}{k} \binom{m}{l}$$
$$\times (-H_1^{\mp})^{m-k} (-H_2^{\pm})^{m-l}$$
$$\times \int \rho^{k+l} \exp[-A\rho^2] \exp[\pm i(l-k)\phi] \rho d\rho d\phi. \tag{23}$$

The integral over ϕ results in a Kronecker delta, $2\pi\delta_{lk}$. Summing over l then reduces the double sum to a single sum, with $l = k$. The cross-spectral density then appears as

$$W(\mathbf{r}_1, \mathbf{r}_2) = 2\pi D(\mathbf{r}_1, \mathbf{r}_2) \sum_{l=0}^{m} \binom{m}{l}^2 (-H_1^{\mp})^{m-l} (-H_2^{\pm})^{m-l}$$
$$\times \int_0^{\infty} \rho^{2l+1} \exp[-A\rho^2] d\rho. \tag{24}$$

The remaining integral can be directly related to the Gamma function, so that

$$W(\mathbf{r}_1, \mathbf{r}_2) = 2\pi D(\mathbf{r}_1, \mathbf{r}_2) \sum_{l=0}^{m} \binom{m}{l}^2 (H_1^{\mp})^{m-l} (H_2^{\pm})^{m-l}$$
$$\times \frac{\Gamma(l+1)}{2A^{l+1}}, \tag{25}$$

where $\Gamma(l + 1)$ is the Gamma function.

In this form, it is difficult to see the functional dependence, as $H_j^{\pm}$ also depends on the position vectors $\mathbf{r}_1$ and $\mathbf{r}_2$. It is readily found, however, that we may write

$$H_2^{\pm} = \left[1 - \frac{1}{\sigma^2 A}\right](x_2 \pm iy_2) - \frac{1}{\tilde{\sigma}^2 A}(x_1 \pm iy_1), \tag{26}$$

with a similar expression for $H_1^{\mp}$. We may finally write a complete expression for the cross-spectral density of a PCVB of any azimuthal order as

$$W(\mathbf{r}_1, \mathbf{r}_2) = \pi D(\mathbf{r}_1, \mathbf{r}_2) \left\{ \sum_{l=0}^{m-1} \binom{m}{l}^2 \frac{\Gamma(l+1)}{A^{2m-l+1}} \right.$$
$$\times \left[\frac{1}{\tilde{\alpha}^2}(x_2 \pm iy_2) - \frac{1}{\tilde{\sigma}^2}(x_1 \pm iy_1)\right]^{m-l}$$
$$\times \left[\frac{1}{\alpha^2}(x_1 \mp iy_1) - \frac{1}{\sigma^2}(x_2 \mp iy_2)\right]^{m-l}$$
$$\left. + \frac{\Gamma(m+1)}{A^{m+1}} \right\}, \tag{27}$$

where

$$\frac{1}{\alpha^2} \equiv \left[\frac{1}{\sigma^2} + \frac{1}{\delta^2}\right]. \tag{28}$$

Equation (27) is the main result of this paper. It is an analytic expression for an entire class of partially coherent vortex beams of any azimuthal order, at any propagation distance.

We may make a few basic observations from this result. First, it can be straightforwardly shown that the exponential factor $D(\mathbf{r}_1, \mathbf{r}_2)$ may be rewritten as

$$D(\mathbf{r}_1, \mathbf{r}_2) = \frac{|C|^2}{\pi\delta^2} \exp\left[-\frac{\rho_2^2}{A\sigma^2\delta^2}\right] \exp\left[-\frac{\rho_1^2}{A\tilde{\sigma}^2\delta^2}\right]$$
$$\times \exp\left[-\frac{|\boldsymbol{\rho}_1 - \boldsymbol{\rho}_2|^2}{A|\sigma|^4}\right]. \tag{29}$$

This indicates that the exponential factors have the form of a Gaussian–Schell model beam (Section 5.3.1 of [25]), in which the spatial coherence depends only on the difference between the two points $\mathbf{r}_1$ and $\mathbf{r}_2$. However, the cross-spectral density in its entirety, represented by Eq. (27), is not Schell model, due to the vortex terms.

The correlation length of the beam can be estimated from the scaling factor $1/\Delta^2 \equiv 1/A|\sigma|^4$ of Eq. (29), which in the plane $z = 0$ takes on the simple form

$$\Delta^2 = 2w_z^2 + \frac{w_z^4}{\delta^2}. \tag{30}$$

For small values of δ, the correlation length is approximately $\Delta \sim w_z^2/\delta$, demonstrating the inverse relation between beam wander and coherence.

It is to be noted that the correlation length has a minimum limiting value given by $2w_z^2$ as $\delta \to \infty$ in this model. This lower limit arises because the partially coherent field is constructed from coherent beams of effective width $2w_z^2$. Beams with a smaller correlation length can be made by simply using a smaller width beam in the beam wander model.

If $m = 1$, our expression for the cross-spectral density reduces to

$$W(\mathbf{r}_1, \mathbf{r}_2) = \frac{\pi D(\mathbf{r}_1, \mathbf{r}_2)}{A^3} \left\{ \left[\frac{1}{\tilde{\alpha}^2} (x_2 \pm iy_2) - \frac{1}{\tilde{\sigma}^2} (x_1 \pm iy_1) \right] \right.$$
$$\left. \times \left[\frac{1}{\alpha^2} (x_1 \mp iy_1) - \frac{1}{\sigma^2} (x_2 \mp iy_2) \right] + 2A \right\}. \quad \textbf{(31)}$$

This expression agrees with Eq. (10) of [20], which was the original derivation of the $m = 1$ case.

If $m = 0$, we are looking at the wandering of a fundamental, non-vortex Gaussian mode. Our expression reduces to

$$W(\mathbf{r}_1, \mathbf{r}_2) = \frac{\pi D(\mathbf{r}_1, \mathbf{r}_2)}{A}. \quad \textbf{(32)}$$

This is, as can be seen simply from Eq. (29), a Gaussian–Schell model beam.

We are now interested in studying how the vortex structure of coherent vortex beams is conveyed to the correlation function when the spatial coherence of the beam is reduced or, equivalently, the beam is allowed to further wander. Correlation vortices exist at those pairs of points $\mathbf{r}_1$ and $\mathbf{r}_2$ for which $\mathrm{Re}\{W\} = 0$ and $\mathrm{Im}\{W\} = 0$. We next study the behavior of such singularities in detail.

3. PROJECTIONS OF SINGULARITIES

Even when considered only in a transverse plane, it is difficult to visualize the behavior of correlation singularities because they depend on two transverse position vectors, $\mathbf{r}_1$ and $\mathbf{r}_2$, and thus four variables. It is therefore often convenient to hold one of the position vectors constant, to be called the fixed point, and to plot the phase in the two variables of the other. This projection of the correlation function allows us to obtain a clear picture of the characteristics of any singularities for a variety of conditions.

We begin by considering the behavior of an $m = 3$ PCVB and its associated singularities as the coherence decreases, as illustrated in Fig. 1. In this figure, and those that follow, we consider the field in the waist plane $z = 0$. Figs. 1(a), 1(c), and 1(e) show the color-coded phase of the correlation function as δ increases. However, as it is sometimes difficult to spot the vortex core in these color plots, the zeros of the real and imaginary parts of the cross-spectral density are shown in Figs. 1(b), 1(d), and 1(f); crossings of these zero lines represent vortices. The fixed point is taken to reside along the y axis.

For a highly coherent beam, Figs. 1(a) and 1(b), there is effectively a single third-order vortex at the origin, as would be expected for a fully coherent beam. The phase increases by 6π, or three 2π increases, as one follows a closed counter-clockwise path around the origin.

As the coherence decreases, Figs. 1(c) and 1(d), the central singularity separates into three first-order singularities, all residing along the y axis. This breakup is expected, as it is well-known that only first-order singularities are stable under wave-field perturbations; such perturbations include a decrease in coherence. The singularities reside along the y axis because the fixed point is on that axis, and the fixed point provides the only break in the rotational symmetry of the problem.

As the coherence further decreases, Figs. 1(e) and 1(f), new singularities appear, of equal and opposite signs of the original singularities, coming in from the point at infinity. As optical vortices themselves do not possess any energy or inertia, they
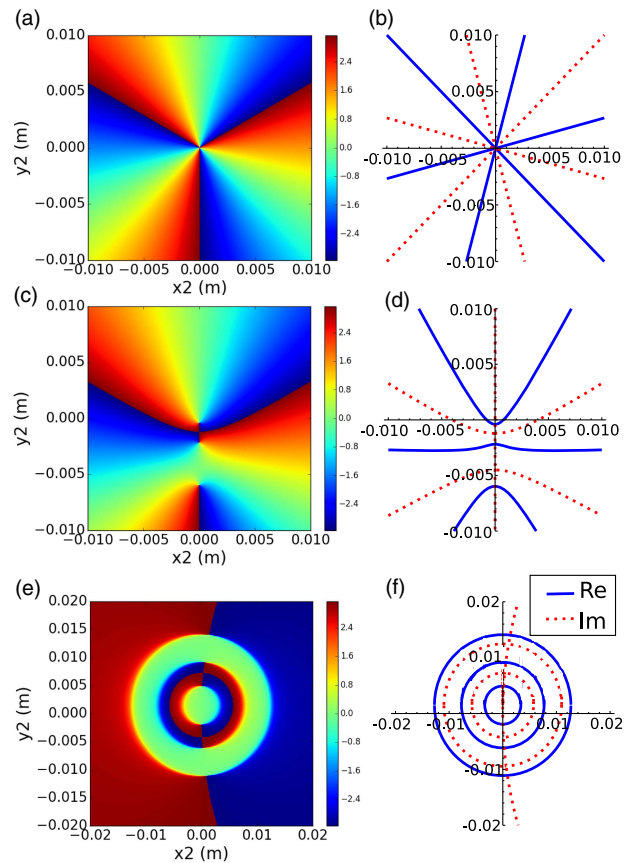
Fig. 1. Phase of the cross-spectral density of a PCVB with $m = 3$. For each of the images above, the beam waist $w_0 = 5$ mm, $\lambda = 500$ nm, $(x_1, y_1) = (0.0, 0.001)$ m, and $m = 3$. Phase plot for a beam with (a) $\delta = 0.00001$ m, (c) $\delta = 0.001$ m, (e) $\delta = 0.1$ m. Real and imaginary parts with locations of vortices circled for beam with (b) $\delta = 0.00001$ m, (d) $\delta = 0.001$ m, (f) $\delta = 0.1$ m.

are able to move, in essence, "infinitely fast," coming from infinity to a finite distance with a finite change in coherence. In the low-coherence limit, the equiphase contours around each vortex compress, resulting in two step-like jumps of π, as one goes around a vortex instead of a smooth 2π ramp.

The existence of these vortices can be seen in Eq. (27), which indicates that the cross-spectral density contains a $2m$th-order polynomial in $z_2 = x_2 + iy_2$ or alternatively can be thought to be an mth-order polynomial in z_2 and an mth-order polynomial in $\tilde{z}_2$. We expect there to be $2m$ distinct roots to this polynomial, which suggests $2m$ vortices, m of which are left-handed and m of which are right-handed.

It is striking that, in Fig. 1(f), we see that the vortices do not in fact reside along a straight line but instead reside on circles formed by circular real and imaginary zeros of the cross-spectral density. This is distinct from the $m = 1$ case, discussed in [21], in which it was shown that, in the waist plane of the beam, the two correlation vortices reside along a straight line, which intersects the origin. It can be shown in Eq. (27) that this is only approximately true for the $|m| > 1$ case when the field is highly coherent. The circles associated with the zero of the real part of the cross-spectral density can be found by taking the limit

$\delta \to \infty$ in Eq. (27); with some effort, one arrives at the following expression for the cross-spectral density:

$$W(\mathbf{r}_1, \mathbf{r}_2) = \pi D(\mathbf{r}_1, \mathbf{r}_2) \frac{w_z^{2m+2}}{2^{m+1}} \left\{ \sum_{l=0}^{m-1} \binom{m}{l}^2 \Gamma(l+1) \right.$$

$$\left. \times (-1)^{m-l} |z_2 - z_1|^{2(m-l)} + \Gamma(m+1) \right\}, \qquad (33)$$

where we have used $z_1 = x_1 \pm i y_1$, and so forth, for brevity. This expression is completely real-valued and is a $2m$th-order polynomial in $|z_2 - z_1|$, indicating that the $2m$ zeros of the real part of $W(\mathbf{r}_1, \mathbf{r}_2)$, with respect to $\mathbf{r}_2$, reside on circles centered on $\mathbf{r}_1$.

The zeros of the imaginary part of $W(\mathbf{r}_1, \mathbf{r}_2)$ come from returning to Eq. (27) and keeping the lowest-order terms with respect to $1/\delta^2$. The condition for the imaginary part of $W(\mathbf{r}_1, \mathbf{r}_2)$ to vanish is then of the form

$$\frac{y_1}{x_1} = \frac{y_2}{x_2}, \qquad (34)$$

or that the zeros with respect to $\mathbf{r}_2$ reside approximately on a straight line going through the point $\mathbf{r}_1$ and the origin. When higher-order terms of $1/\delta^2$ are included, this straight line becomes curved.

It should be noted that the circles of Eq. (33) have finite radii as $\delta \to \infty$; we interpret this as a consequence of the fact that the correlation length of the field never approaches zero, as indicated by Eq. (30). This suggests that a more advanced model of partially coherent vortex beams will be needed to study the effect of low spatial coherence of vortices. We also note that the position of the vortices changes in a nontrivial way when the field propagates, as was discussed for the $m = 1$ case in [22].
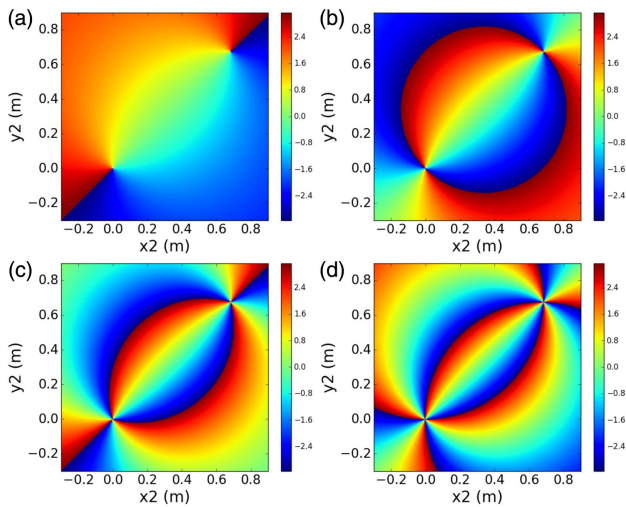
Fig. 2. Phase of the cross-spectral density of a PCVB of different vortex orders. For each of the images above, the beam waist $w_0 = 5$ mm, $\lambda = 500$ nm, $(x_1, y_1) = (0.001, 0.001)$ m, and $\delta = 0.001$ m. (a) $m = 1$, (b) $m = 2$, (c) $m = 3$, (d) $m = 4$. The pairs of clockwise and anticlockwise vortices can be seen to lie approximately along the line $x = y$. For every increase in order, another pair is formed.

A detailed view of the equal and opposite sets of vortices can be seen for different values of m in Fig. 2. Now all the vortices reside approximately along a diagonal line running through the origin, as the fixed point has been placed on the diagonal. In this larger transverse cross-section of the beam, the individual groups of positive and negative vortices each appear in the figure as a single high-order vortex.

It is to be noted that it is necessary to have the fixed point displaced from the central beam axis if vortices are to be observed. When $\mathbf{r}_1$ resides directly on axis, the system is completely rotationally symmetric with respect to $\mathbf{r}_2$, and the only singularities observed are zero circles, known as ring dislocations, as seen in [14].

4. TOPOLOGICAL CHARGE

As seen in previous examples, the phase always changes by an integer multiple of 2π when one follows a closed counterclockwise trajectory around a vortex; this integer is known as the topological charge. It can be shown that the net topological charge of a vortex beam is in general conserved, and typically vortices only appear or disappear in pairs of equal and opposite charge that conserves the net charge. These properties of vortices, discreteness, and stability make them of interest for free-space optical communications because they indicate that a vortex might be a turbulence-resistant carrier of information [26]. However, we have seen from examples such as in Fig. 2 that the net topological charge of a PCVB evidently decreases as the coherence is decreased; here we quantify this effect.

It is to be noted that there are two possible ways to describe the topological charge of the PCVBs considered here. Provided the field fluctuations are slow enough, the instantaneous topological charge within an aperture could be measured and the average value calculated. Using the beam wander model, the measured topological charge will be m if $\mathbf{r}_0$ resides within a circular aperture A of radius a and 0 if $\mathbf{r}_0$ resides outside the aperture. The average topological charge $\bar{t}$ of a beam will be given by

$$\bar{t} = m \int_A f(\mathbf{r}_0) d^2 r_0 = m[1 - \exp(-a^2/\delta^2)]. \qquad (35)$$

If $\delta = 0$, $\bar{t} = m$ and if $\delta \to \infty$, $\bar{t} \to 0$.

Typically, however, we might expect the fluctuations of the field to be too fast to directly measure; in such a situation, we can only measure the topological charge of the cross-spectral density. To do so, one must choose a fixed point $\mathbf{r}_1$ and determine the charge with respect to the point $\mathbf{r}_2$.

Figure 3 shows the topological charge of PCVBs of three different orders as a function of δ. The topological charge is calculated within a circular aperture of radius $a = 1$ cm, and the loss of charge is shown for two different positions of the fixed point in Figs. 3(a) and 3(b).

It can be seen that, as δ increases and coherence therefore decreases, the topological charge is lost in discrete drops. Evidently the charge is more robust for a fixed point farther away from the origin, but it is still lost even with a wander parameter δ much smaller than the aperture size. Higher-order beams maintain some amount of charge longer than lower-order beams, while lower order beams maintain their initial
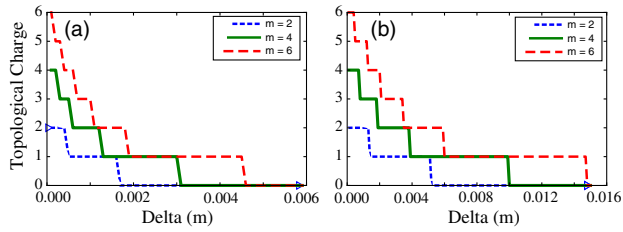
Fig. 3. Topological charge of a PCVB as a function of beam wander. The beam waist $w_0 = 5$ mm, and $\lambda = 500$ nm. The detector radius was set at 1 cm. As δ increases, the coherence of the beam decreases, and the detectable topological charge drops. (a) $(x_1, y_1) = (.0001, .0001)$ m, (b) $(x_1, y_1) = (.001, .001)$ m. Shifting the fixed point farther away from the origin has the same effect as increasing the coherence.

charge for higher values of δ. This result suggests that the use of vortices and partial coherence together in any application will naturally involve a trade-off: though partially coherent beams typically propagate through the atmosphere with smaller intensity fluctuations than their fully coherent counterparts; these beams also will typically start out with a topological charge reduced from the fully coherent case. The optimal balance of vortex and coherence properties will no doubt depend on the specifics of the application.

We have already seen that this loss of topological charge can be attributed to the appearance of oppositely charged vortices from infinity. An alternative way to explain the effect, perhaps more readily understandable, is to return to the beam wander model. As the coherence is decreased, and the beam is allowed to wander more from the central axis, it will spend more time with its vortex lying outside of the region of the aperture and remain undetectable. One would expect that the topological charge of the cross-spectral density would therefore also be reduced, similar to the loss that appears in Eq. (35).

5. ORBITAL ANGULAR MOMENTUM

It has long been known [27] that a vortex structure in an optical beam is associated with the orbital angular momentum (OAM) of the beam, though it is also known that the relationship between vortices and OAM is only simple in the case of pure vortex beams [28]. We conclude this paper by studying how the OAM of PCVBs depend on the state of coherence.

The physical quantity of relevance is the z component of the orbital angular momentum flux density flowing across a plane of constant z, which represents the flux density of OAM as a function of position in the cross section of the beam. For a partially coherent field, this flux density may be expressed as [29]

$$L_{\text{orbit}}(\mathbf{r}, \mathbf{r}', \omega) = -\frac{\varepsilon_0}{2k} \text{Im} \left\{ y \frac{\partial}{\partial x'} W_{yy}(\mathbf{r}, \mathbf{r}', \omega) \right.$$
$$- x \frac{\partial}{\partial y'} W_{yy}(\mathbf{r}, \mathbf{r}', \omega) - x \frac{\partial}{\partial y'} W_{xx}(\mathbf{r}, \mathbf{r}', \omega)$$
$$\left. + y \frac{\partial}{\partial x'} W_{xx}(\mathbf{r}, \mathbf{r}', \omega) \right\}_{r=r'}. \quad (36)$$

(The analogous expression in Ref. [29] contained a sign error that has been corrected here.) For an unpolarized beam with $W_{xx} = W_{yy} = W$, the expression simplifies to

$$L_{\text{orbit}}(\mathbf{r}, \omega) = \frac{-\epsilon_0}{k} \text{Im} \left\{ y \frac{\partial}{\partial x'} W(\mathbf{r}, \mathbf{r}', \omega) - x \frac{\partial}{\partial y'} W(\mathbf{r}, \mathbf{r}', \omega) \right\}_{r=r'}. \quad (37)$$

On substitution from Eq. (27) into Eq. (37), we have

$$L_{\text{orbit}}(\mathbf{r}, \omega) = \beta \frac{\pi \epsilon_0}{k} \exp[-2r^2/w_z^2\beta] \times \sum_{n}^{m-1} C_n^m (m - n) r^{2(m-n)}, \quad (38)$$

where we have defined

$$C_n^m \equiv \binom{m}{n}^2 \frac{|C|^2}{\pi \delta^2} \frac{\Gamma(n + 1)}{A^{n+1}} \beta^{-2(m-n)}, \quad (39)$$

with

$$\beta \equiv \left(1 + \frac{2\delta^2}{w_z^2} \right), \quad (40)$$

and $r = \sqrt{x^2 + y^2}$.

This unnormalized quantity depends on the intensity of the light beam as well as the density of angular momentum. We may define a normalized orbital angular momentum flux density, which roughly describes the orbital angular momentum per photon of a vortex beam as a function of radial position,

$$l_{\text{orb}}(\mathbf{r}, \omega) = \frac{\hbar \omega L_{\text{orbit}}(\mathbf{r}, \omega)}{S(\mathbf{r}, \omega)}, \quad (41)$$

where $S(\mathbf{r}, \omega)$ is the z component of the Poynting vector,

$$S(\mathbf{r}, \omega) = \frac{k}{\mu_0 \omega} W(\mathbf{r}, \mathbf{r}, \omega) \quad (42)$$

$$= \frac{\pi k}{\mu_0 \omega} \exp[-2r^2/w_z^2\beta] \sum_{n=0}^{m} C_n^m r^{2(m-n)}. \quad (43)$$

With a small amount of effort, the normalized OAM flux density can be shown to be of the form

$$l_{\text{orb}}(\mathbf{r}, \omega) = \hbar \beta \frac{\sum_{n=0}^{m-1} C_n^m (m - n) r^{2(m-n)}}{\sum_{n=0}^{m-1} C_n^m r^{2(m-n)} + C_m^m}. \quad (44)$$

From this expression, the behavior of the angular momentum density as a function of vortex order can be evaluated. For small values of r, the expression takes on the approximate form

$$l_{\text{orb}}(r, \omega) \approx \hbar \left(1 + \frac{2\delta^2}{w_z^2} \right) \frac{C_{m-1}^m r^2}{C_m^m}, \quad (45)$$

behaving in a roughly quadratic fashion, while for larger values of r, the effect of the C_m is negligible, and the value approaches a constant value of

$$l_{\text{orb}}(r, \omega) \approx m \hbar \left(1 + \frac{2\delta^2}{w_z^2} \right). \quad (46)$$

Taken together this describes a Rankine vortex, already discussed for the first order case in [29,30]; an illustration of the OAM flux density as a function of radial position for different values of δ is shown in Fig. 4. There are several features of interest here. As can be seen from Eq. (46) or from Fig. 4(a), the
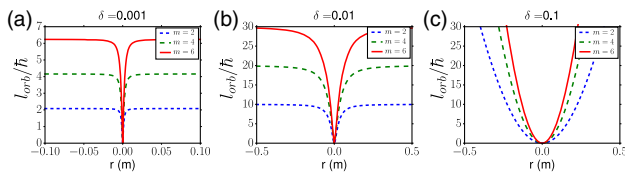
Fig. 4. Normalized orbital angular momentum flux density for different states of coherence. For each of the images above, the beam waist $w_0 = 5$ mm and $\lambda = 500$ nm. (a) $\delta = 0.001$ m, (b) $\delta = 0.01$ m, (c) $\delta = 0.1$ m. Note the increasing range required to view the Rankine vortex structure as the coherence decreases.

value of the OAM at large r increases by integer multiples of the OAM of a first order ($m = 1$) beam for a highly coherent beam. Additionally, a highly coherent beam acts much like a pure fluid-like rotator (angular momentum independent of radial distance), while a highly incoherent field acts much like a pure rigid-body rotator (angular momentum is quadratic with radial distance). By decreasing the spatial coherence of a vortex beam, one can increase the density of orbital angular momentum at the fringes of the beam, at the cost of reducing it dramatically at the beam center.

6. CONCLUSION

In this paper, we have laid out a complete description of a new class of beam: the partially coherent vortex beam constructed from randomized Laguerre–Gauss beams. This class of beams has a fully analytic form with a regular, predictable behavior that does not rely on computational methods for study. Each order of the beam increases the orbital angular momentum by an integer multiple of the orbital angular momentum of the first order, and the topological charge is detectable for beams with a coherence parameter $\delta < 0.0001$ m. With this improved understanding, researchers are now better equipped to make use of this beam class in a variety of applications.

REFERENCES

1. M. Soskin and M. Vasnetsov, "Singular optics," in *Progress in Optics*, E. Wolf, ed. (Elsevier, 2001), Vol. **42**, p. 219.
2. M. Dennis, K. O'Holleran, and M. Padgett, "Singular optics: optical vortices and polarization singularities," in *Progress in Optics*, E. Wolf, ed. (Elsevier, 2009), Vol. **53**, p. 293.
3. N. Simpson, K. Dholakia, L. Allen, and M. Padgett, "Mechanical equivalence of spin and orbital angular momentum of light: an optical spanner," Opt. Lett. **22**, 52–54 (1997).
4. J. H. Lee, G. Foo, E. G. Johnson, and G. A. Swartzlander, Jr., "Experimental verification of an optical vortex coronagraph," Phys. Rev. Lett. **97**, 053901 (2006).
5. D. Palacios, D. Rozas, and G. A. Swartzlander, Jr., "Observed scattering into a dark optical vortex core," Phys. Rev. Lett. **88**, 103902 (2002).
6. A. Jesacher, S. Fürhapter, S. Bernet, and M. Ritsch-Marte, "Shadow effects in spiral phase contrast microscopy," Phys. Rev. Lett. **94**, 233902 (2005).
7. G. Gibson, J. Courtial, M. J. Padgett, M. Vasnetsov, V. Pas'ko, S. M. Barnett, and S. Franke-Arnold, "Free-space information transfer using light beams carrying orbital angular momentum," Opt. Express **12**, 5448–5456 (2004).
8. Y. Gu and G. Gbur, "Reduction of turbulence-induced scintillation by nonuniformly polarized beam arrays," Opt. Lett. **37**, 1553–1555 (2012).
9. L. M. Narducci and J. D. Farina, "An investigation of variable coherence sources & of some practical applications," Technical Report, DTIC Document (1981).
10. E. Wolf, "Significance and measurability of the phase of a spatially coherent optical field," Opt. Lett. **28**, 5–6 (2003).
11. H. F. Schouten, G. Gbur, T. D. Visser, and E. Wolf, "Phase singularities of the coherence functions in Young's interference pattern," Opt. Lett. **28**, 968–970 (2003).
12. I. Freund, "Bichromatic optical lissajous fields," Opt. Commun. **226**, 351–376 (2003).
13. I. D. Maleev and G. A. Swartzlander, Jr., "Propagation of spatial correlation vortices," J. Opt. Soc. Am. B **25**, 915–922 (2008).
14. D. Palacios, I. Maleev, A. Marathay, and G. Swartzlander, Jr., "Spatial correlation singularity of a vortex field," Phys. Rev. Lett. **92**, 143905 (2004).
15. W. Wang, Z. Duan, S. G. Hanson, Y. Miyamoto, and M. Takeda, "Experimental study of coherence vortices: local properties of phase singularities in a spatial coherence function," Phys. Rev. Lett. **96**, 073902 (2006).
16. Y. Yang, M. Chen, M. Mazilu, A. Mourka, Y.-D. Liu, and K. Dholakia, "Effect of the radial and azimuthal mode indices of a partially coherent vortex field upon a spatial correlation singularity," New J. Phys. **15**, 113053 (2013).
17. B. Perez-Garcia, A. Yepiz, R. I. Hernandez-Aranda, A. Forbes, and G. A. Swartzlander, "Digital generation of partially coherent vortex beams," Opt. Lett. **41**, 3471–3474 (2016).
18. G. Gbur and T. D. Visser, "Phase singularities and coherence vortices in linear optical systems," Opt. Commun. **259**, 428–435 (2006).
19. G. Gbur and T. D. Visser, "Coherence vortices in partially coherent beams," Opt. Commun. **222**, 117–125 (2003).
20. G. Gbur, T. D. Visser, and E. Wolf, "'Hidden' singularities in partially coherent wavefields," J. Opt. A **6**, S239–S242 (2004).
21. G. Gbur and G. A. Swartzlander, Jr., "Complete transverse representation of a correlation singularity of a partially coherent field," J. Opt. Soc. Am. B **25**, 1422–1429 (2008).
22. C. Stahl and G. Gbur, "Complete representation of a correlation singularity in a partially coherent beam," Opt. Lett. **39**, 5985–5988 (2014).
23. F. Wang, Y. Cai, and O. Korotkova, "Partially coherent standard and elegant Laguerre–Gaussian beams of all orders," Opt. Express **17**, 22366–22379 (2009).
24. E. Wolf, "New theory of partial coherence in the space-frequency domain. Part I: spectra and cross spectra of steady-state sources," J. Opt. Soc. Am. A **72**, 343–351 (1982).
25. E. Wolf, *Introduction to the Theory of Coherence and Polarization of Light* (Cambridge University, 2007).
26. G. Gbur and R. K. Tyson, "Vortex beam propagation through atmospheric turbulence and topological charge conservation," J. Opt. Soc. Am. A **25**, 225–230 (2008).
27. L. Allen, M. W. Beijersbergen, R. Spreeuw, and J. Woerdman, "Orbital angular momentum of light and the transformation of Laguerre–Gaussian laser modes," Phys. Rev. A **45**, 8185–8189 (1992).
28. M. Berry, "Paraxial beams of spinning light," Proc. SPIE **3487**, 6–11 (1998).
29. S. Kim and G. Gbur, "Angular momentum conservation in partially coherent wave fields," Phys. Rev. A **86**, 043814 (2012).
30. G. A. Swartzlander, Jr. and R. I. Hernandez-Aranda, "Optical Rankine vortex and anomalous circulation of light," Phys. Rev. Lett. **99**, 163901 (2007).